Geochemistry Geophysics Geosystems G3

Article
Volume 12, Number 10
20 October 2011
Q10011, doi:10.1029/2011GC003700
ISSN: 1525-2027

Published by AGU and the Geochemical Society

The plutonic record of a silicic ignimbrite from the Latir volcanic field, New Mexico

Michael J. Tappa
Department of Geological Sciences, University of North Carolina, Mitchell Hall, Chapel Hill, North Carolina 27599-3315, USA

Now at Jacobs Technology, ESCG, NASA Johnson Space Center, Houston, Texas 77058-3607, USA

Drew S. Coleman and Ryan D. Mills
Department of Geological Sciences, University of North Carolina, Mitchell Hall, Chapel Hill, North Carolina 27599-3315, USA (dcoleman@unc.edu)

Kyle M. Samperton
Department of Geological Sciences, University of North Carolina, Mitchell Hall, Chapel Hill, North Carolina 27599-3315, USA

Now at Department of Geosciences, Princeton University, Guyot Hall, Princeton, New Jersey 08544-1003, USA

[1] Zircon U-Pb geochronologic data for plutonic rocks in the Latir volcanic field, New Mexico, demonstrate that the rocks are dominated by plutons that post-date ignimbrite eruption. Only zircon from the ring dike of the Questa caldera yields the same age (25.64 ± 0.08 Ma) as zircon from the caldera-forming Amalia Tuff (25.52 ± 0.06 Ma). The post-caldera Rio Hondo pluton was assembled incrementally over at least 400 ka. The magma accumulation rate for the exposed portion of the Rio Hondo pluton is estimated to be 0.0003 $km^3\ a^{-1}$, comparable to rates for other plutons, and too slow to support accumulation of large eruptible magma volumes. Extrapolation of the accumulation rate for the Rio Hondo pluton over the history of the Latir volcanic field yields an estimated volume of plutonic rocks comparable to the calculated volume under the field as determined by geophysical studies. We propose that the bulk of the plutonic rocks beneath the volcanic center accumulated during periods of low volcanic effusivity. Furthermore, because the oldest portion of the Rio Hondo pluton is the granitic cap exposed beneath a gently dipping roof contact, the roof granite cannot be a silicic liquid fractionated from the deeper (younger) portions of the pluton. Instead, our data suggest that the compositional heterogeneity of the Rio Hondo pluton is inherited from lower crustal sources. We suggest that if magma fluxes are high enough, zoned ignimbrites can be formed by evolution of the melt compositions generated at the source with little or no shallow crustal differentiation.

Components: 10,700 words, 3 figures, 1 table.

Keywords: pluton-ignimbrite connections.

Index Terms: 1036 Geochemistry: Magma chamber processes (3618); 3643 Mineralogy and Petrology: Layered magma chambers; 8035 Structural Geology: Pluton emplacement.

Received 16 May 2011; **Revised** 7 September 2011; **Accepted** 9 September 2011; **Published** 20 October 2011.

Tappa, M. J., D. S. Coleman, R. D. Mills, and K. M. Samperton (2011), The plutonic record of a silicic ignimbrite from the Latir volcanic field, New Mexico, *Geochem. Geophys. Geosyst.*, *12*, Q10011, doi:10.1029/2011GC003700.

1. Introduction

[2] Debate persists as to the nature of the relationship between plutonic and volcanic rocks. Opposing views posit that either plutonic rocks comprise unerupted crystal and liquid residua of volcanic eruptions, and are thus geochemically complementary to volcanic rocks [*Hildreth*, 2004; *Eichelberger et al.*, 2006; *Bachmann et al.*, 2007; *Lipman*, 2007; *de Silva and Gosnold*, 2007], or that plutonic rocks are unerupted, unfractionated equivalents of volcanic rocks [*Glazner et al.*, 2008]. Large-scale (hundreds of km^3) caldera eruptions represent one end-member in the continuum of plutonic-volcanic rock connections because current caldera models predict voluminous pluton formation, up to an order of magnitude larger than the erupted material, during the generation of ignimbrite magmas [e.g., *Lipman*, 2007].

[3] Caldera collapse and ignimbrite eruption are thought to result from the partial evacuation of massive differentiated magma chambers at shallow crustal levels, the crystal-liquid residuum of which is preserved as plutons [*Smith*, 1979; *Lipman*, 1984; *Bachmann and Bergantz*, 2004, 2008a, 2008b; *Hildreth*, 2004; *Lipman*, 2007]. This model is based, in part, on the similarity between zoning of large ignimbrites and zoning of intrusive suites such as the Tuolumne Intrusive Suite of the Sierra Nevada batholith [*Hildreth*, 1981]. However, recently published geochronologic data show that many large plutonic suites were emplaced incrementally over millions of years, at rates far too slow to fractionate the voluminous siliceous cap required by the traditional caldera model for ignimbrite formation [*Coleman et al.*, 2004; *Bartley et al.*, 2005; *Matzel et al.*, 2006; *Davis et al.*, 2011]. *Glazner et al.* [2004] suggested an alternative ignimbrite model that predicts caldera collapse to result from a period of high magma flux to upper crustal levels that may be poorly represented in the plutonic rock record. In this model, an unstable shallow magma body is assembled rapidly and collapses quickly after amalgamation, resulting in nearly complete chamber evacuation and leaving few remnant plutonic rocks [*Roche and Druitt*, 2001; *Glazner et al.*, 2004].

[4] Thus, there are two fundamental differences between the models for formation of ignimbrites. The traditional model predicts massive remnant coeval plutons approximately three to ten times the volume of the ignimbrite [*Smith*, 1979; *Bachmann and Bergantz*, 2004, 2008a, 2008b; *Hildreth*, 2004; *White et al.*, 2006; *Lipman*, 2007]. Furthermore, the pluton and the volcanic rock are complementary residual solid + unerupted liquid, and erupted liquid, respectively. The alternative model predicts ignimbrites to be the erupted products of magma chambers that are comparable in size to the erupted material, and that erupt nearly completely, leaving little plutonic residue. This model also predicts that any residual plutonic rocks would be compositionally equivalent to the erupted volcanic material.

[5] Because estimates of the flux of magma into the shallow crust are key to testing ignimbrite formation models [e.g., *Annen*, 2009], high-precision geochronologic data have become important to evaluating pluton/ignimbrite connections. *Petford et al.* [2000] estimated fluxes for filling plutons from 0.0001 to 1 $km^3\ a^{-1}$ by considering the physical problem of moving a granitic melt through the crust. Thermal modeling by *Annen* [2009] demonstrates that magma fluxes at the upper end of this range (rates >0.01 $km^3\ a^{-1}$) are necessary to develop eruptible volumes of magma that are comparable to large ignimbrite eruptions (>400 km^3). This may be broadly supported by estimates of accumulation for two well-dated ignimbrites. Using an erupted volume of 5000 km^3 for the Fish Canyon Tuff [*Lipman*, 2000] and a total age range of zircon in the tuff of 500 ka [*Schmitz and Bowring*, 2001] yields a magma flux of 0.01 $km^3\ a^{-1}$. Similarly, the 600 km^3 Bishop Tuff with a total zircon age range of 65 ka [*Simon and Reid*, 2005; *Crowley et al.*, 2007] yields a flux of approximately 0.01 $km^3\ a^{-1}$. These estimates are likely minima because the maximum range of all analyzed zircon was used to calculate flux (i.e., assuming no spread in ages as a result of inherited grains, Pb-loss, or analytical variability). Furthermore, if the erupted material represents only 10–30% of the magma system, flux estimates increase accordingly. In contrast, estimates of pluton filling rates made using high-precision U-Pb zircon geochronology are more in line with the lower end of *Petford et al.*'s [2000] range, and are on the order of 0.0001 to 0.01 $km^3\ a^{-1}$ [*Coleman et al.*, 2004; *Matzel et al.*, 2006; *Michel et al.*, 2008].

[6] The competing hypotheses for pluton/ignimbrite connections could be tested by dating the plutons and ignimbrite from a single caldera to identify coeval intrusive and extrusive rocks, and further by comparing magma flux for plutons that are coeval with the ignimbrite. However, this requires exposure

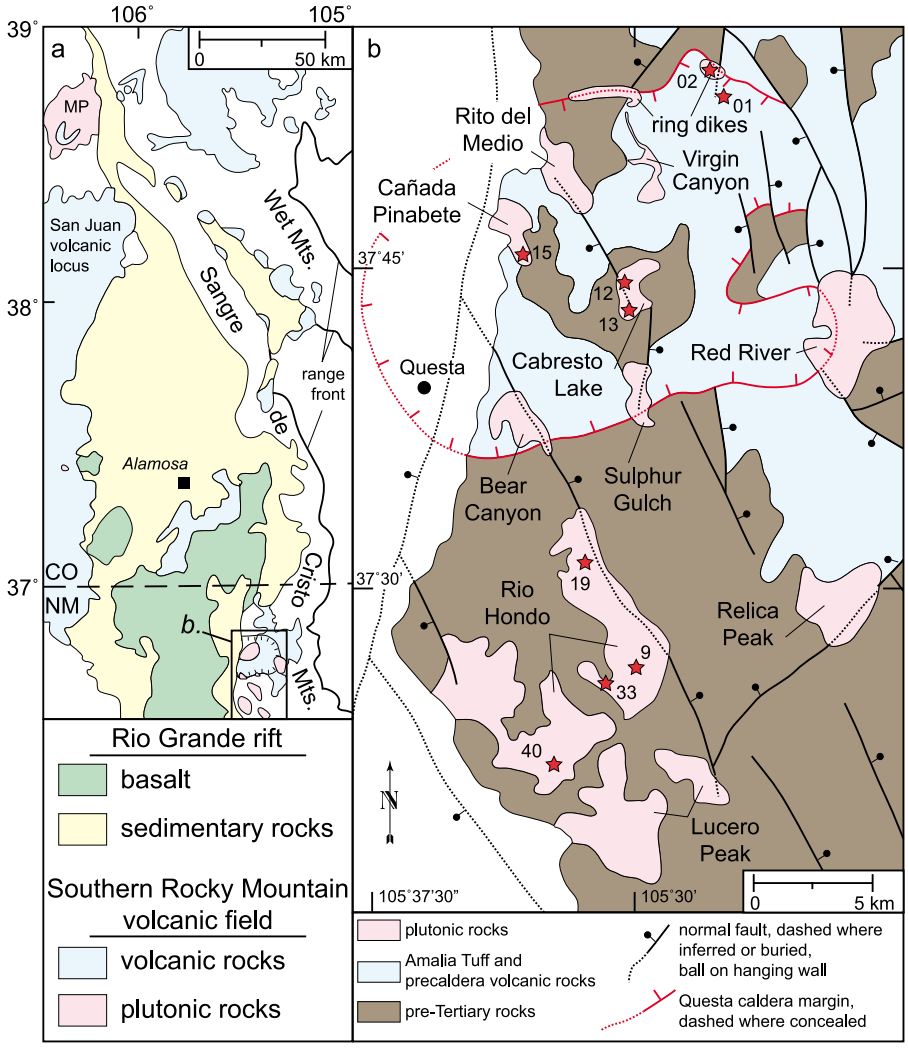

Figure 1. Simplified geologic map of (a) the northern Rio Grande rift [after *Lipman*, 2007] and (b) Questa caldera (modified from *Lipman and Reed* [1989]). Location of area enlarged in Figure 1b is indicated in Figure 1a. In Figure 1a, Rio Grande rifting has exposed the plutonic roots of Oligo-Miocene calderas associated with the Southern Rocky Mountain volcanic field. Large pluton in north (MP) is the Mount Princeton batholith, and volcanic field on the western side is the eastern edge of the San Juan volcanic locus from which the Fish Canyon tuff erupted. In Figure 1b, approximate locations of samples dated are indicated by sample ID suffix only (eg., AT09–01 is labeled "01"). Ring dikes at the northern caldera margin are peralkaline granite. Although not considered part of the Virgin Canyon pluton by *Lipman and Reed* [1989] they are compositionally the same as the peralkaline marginal unit of the pluton and closely associated with it.

of both plutonic and volcanic components of the same caldera system, and such exposures are rare. In the Southern Rocky Mountain volcanic field of Colorado and New Mexico, USA, late Eocene through early Miocene calderas were dissected by normal faulting associated with opening of the Rio Grande Rift (Figure 1a). Normal faulting near the Questa caldera resulted in the exposure of shallow levels of plutonic rocks and volcanic rocks associated with caldera formation, thus allowing for the temporal comparison between the two rock types from the same magmatic system.

2. Geologic Background

[7] The Questa caldera, located in the Latir volcanic field of north-central New Mexico, formed in response to eruption of the Amalia Tuff [*Lipman et al.*, 1986] at approximately 25.39 ± 0.04 Ma (M. J. Zimmerer and W. C. McIntosh, The Ar/Ar

geo- and thermochronology of the Latir volcanic field and the associated intrusions: Understanding caldera magmatic processes using the volcanic-plutonic relationship, submitted to *Geological Society of America Bulletin*, 2011) (Figure 1b). Normal faulting associated with the Rio Grande rift began at approximately 15 Ma, and resulted in several kilometers of relief along the main rift escarpment [*Chapin*, 1979; *Tweto*, 1979], thereby exposing plutonic rocks structurally below the Latir volcanic rocks [*Lipman*, 1984]. Volcanism in the Latir field is categorized into three phases: precaldera, ignimbrite, and postcaldera stages, correlating respectively to the waxing, ignimbrite, and waning stages defined by *Lipman* [2007].

[8] Precaldera volcanism initiated at 28.50 ± 0.19 Ma (Zimmerer and McIntosh, submitted manuscript, 2011) and is dominated by eruption of intermediate magmas [*Lipman et al.*, 1986]. Volcanism climaxed at 25.39 Ma (Zimmerer and McIntosh, submitted manuscript, 2011) with eruption of the ~500 km^3 peralkaline Amalia Tuff, a crystal-poor high-silica rhyolite ignimbrite [*Lipman et al.*, 1986]. Postcaldera volcanism was dominated by intermediate composition volcanic eruptions that are preserved on two intrarift horst blocks west of the Questa caldera [*Thompson et al.*, 1986].

[9] Nine subvolcanic plutons crop out within the Latir field [*Lipman*, 1984] (Figure 1b). Existing geochronologic data suggest that the intrusive rock record is dominated by postcaldera rocks [*Lipman et al.*, 1986; *Czamanske et al.*, 1990; Zimmerer and McIntosh, submitted manuscript, 2011] that can be divided into three groups on the basis of age and spatial proximity [*Lipman et al.*, 1986]. The intracaldera Cañada Pinabete, Virgin Canyon, Rito del Medio and Cabresto Lake plutons form the oldest northern group. The Bear Canyon, Sulphur Gulch, and Red River plutons form the intermediate age caldera margin group. The Rio Hondo and Lucero Peak plutons form the youngest and most southern group. Early $^{40}Ar/^{39}Ar$ [*Czamanske et al.*, 1990], K/Ar, and fission track dates [*Lipman et al.*, 1986] that were used to estimate the timing of intrusions were recently supplanted by detailed $^{40}Ar/^{39}Ar$ thermochronology for all the intrusive rocks (Zimmerer and McIntosh, submitted manuscript, 2011); these more recent dates are therefore used in this study. Unless otherwise indicated, all $^{40}Ar/^{39}Ar$ dates discussed herein are cited from their study.

[10] *Lipman* [1988] identified three phases that comprise the Cañada Pinabete and Virgin Canyon plutons. The oldest phase is a discontinuous ring dike of distinctive peralkaline granite that is compositionally similar to the erupted Amalia Tuff, and interpreted to represent unerupted ignimbrite [*Lipman et al.*, 1986; *Johnson et al.*, 1989]. A compositionally similar unit is in gradational contact with porphyritic metaluminous granite that is intruded by equigranular metaluminous granite in both the Cañada Pinabete and Virgin Canyon plutons. The metaluminous granites are categorized as early and late phases of the same pluton with the early phase being structurally above the late phase [*Lipman*, 1988]. Paleomagnetic and petrologic evidence suggest that the plutons crystallized from the top down [*Hagstrum and Lipman*, 1986; *Johnson et al.*, 1989]. Biotite $^{40}Ar/^{39}Ar$ data for the late metaluminous phase of the Cañada Pinabete yields a plateau age of 25.38 ± 0.09 Ma that is within uncertainty of the age of the Amalia Tuff.

[11] The Rito del Medio pluton (25.19–24.82 Ma: biotite $^{40}Ar/^{39}Ar$ data), is texturally and compositionally similar to the later metaluminous granites of the Cañada Pinabete and Virgin Canyon plutons, and is interpreted to represent the deepest exposures within the caldera [*Lipman*, 1988]. The Cabresto Lake pluton (24.84–24.81 Ma: biotite $^{40}Ar/^{39}Ar$ data) is the most mafic of the intracaldera plutons, but also preserves some compositional zonation from biotite-hornblende monzogranite to silicic granite and aplite [*Lipman*, 1988].

[12] After intrusion of the northern plutons, magmatism shifted toward the southern margin of the caldera [*Lipman et al.*, 1986; *Czamanske et al.*, 1990]. Field relations show that the caldera margin plutons cut the Amalia Tuff [*Lipman*, 1988], consistent with their relatively younger $^{40}Ar/^{39}Ar$ biotite ages for the plutons (24.94–24.37 Ma). The group consists of three lithologically distinct intrusive rock units: the Bear Canyon and Sulfur Gulch plutons and the Red River intrusive complex. The Bear Canyon and Sulfur Gulch plutons are hydrothermally altered high-silica granites, containing zones of molybdenite mineralization.

[13] The Rio Hondo pluton, of the southern pluton group, is the largest exposed intrusive map unit in the Latir field and varies texturally and compositionally from equigranular granite to megacrystic K-feldspar quartz monzonite. The granitic unit is interpreted to represent the cap or roof of a magma chamber, formed by differentiation from the main pluton body [*Lipman et al.*, 1986; *Johnson et al.*, 1989]. The Lucero Peak pluton is the other southern pluton group member and represents the youngest exposed plutonic rock associated with the Latir

volcanic field [*Lipman and Reed*, 1989]. Biotite $^{40}Ar/^{39}Ar$ dates indicate that both the Rio Hondo pluton (21.51–21.22 Ma) and the Lucero Peak pluton (19.34–19.14 Ma) significantly postdate the ignimbrite eruption.

3. Methods

[14] Samples of the Amalia Tuff, the peralkaline granitic ring dike and the Cañada Pinabete, Cabresto Lake and Rio Hondo plutons were collected for zircon U/Pb geochronology. These units were singled out because they offer the best opportunities to compare ages of the tuff and the associated shallow plutonic system (Amalia Tuff, Cañada Pinabete and Cabresto Lake), and evaluate magma flux and differentiation processes (Rio Hondo). The samples are the same as those dated by Zimmerer and McIntosh (submitted manuscript, 2011) for $^{40}Ar/^{39}Ar$ thermochronology cited above.

[15] All samples were crushed using a jaw crusher and a disc mill. Zircon was isolated using standard density (water table and heavy liquids) and magnetic separation techniques. Individual grains were selected using a binocular microscope to represent the range of size and morphology present in the populations. The selected grains were thermally annealed for 48 h at 900°C [*Mattinson*, 2005] and chemically abraded for 12 h at 220°C to remove any domains that experienced Pb loss [*Mundil et al.*, 2004; *Mattinson*, 2005]. Depending on the size of the zircon grains, fractions of 1 to 6 individual grains were selected for analysis. Zircon was dissolved in 29 M HF acid and spiked using a ^{205}Pb-^{233}U-^{236}U tracer [*Krogh*, 1973; *Parrish and Krogh*, 1987]. Anion exchange column chromatography was used to isolate U and Pb from the dissolved solution. Analyses of U and Pb were completed using a VG Sector 54 thermal ionization mass spectrometer (TIMS) at the University of North Carolina - Chapel Hill. Uranium was run as a metal after loading in graphite and H_3PO_4 on single Re filaments. Lead was loaded in silica gel on single Re filaments. Both U and Pb were analyzed in single-collector peak-switching mode using a Daly ion-counting system. Data processing and age calculations were completed using the algorithms of *Ludwig* [1989, 1990] and *Isoplot* v. 3.00 [*Ludwig*, 2003]. Decay constants used are $^{238}U = 1.55125 \times 10^{-10}$ a^{-1} and $^{235}U = 9.8485 \times 10^{-10}$ a^{-1} [*Steiger and Jäger*, 1978]. Corrections for initial Th/U disequilibrium [*Schmitz and Bowring*, 2001] were made using Th and U concentration data for the host plutons [*Johnson et al.*, 1989], following the procedure outlined by *Mattinson* [1973].

4. Results

[16] Zircons from all samples contain few inclusions and lack visible inherited cores as determined following interrogation by cathodoluminescence imaging. After Th correction, all fractions are concordant within uncertainty (considering analytical and decay-constant uncertainties; Table 1). Consequently, we use the weighted mean $^{206}Pb/^{238}U$ age as the best estimate for the crystallization age of the samples (Figure 2). For some samples there is scatter in ages beyond analytical uncertainty, but there is also a cluster of a subset of analyses defined by three or more overlapping data points. For these samples we report the $^{206}Pb/^{238}U$ ages for the entire data set and the subset of overlapping analyses, separately.

[17] Although pooling zircons into multigrain fractions can compress the spread in data and thereby produce apparently precise, but inaccurate, ages [*Renne et al.*, 2006], we adopted a multigrain analytical strategy in order to circumvent the problem of low U concentrations in sampled zircons and maintain high radiogenic Pb:common Pb ratios. Such an approach was particularly necessary for some of the intracaldera samples (Cañada Pinabete and ring dike) that are characterized by both small zircon volume and low U concentration. Nonetheless, we are confident that our weighted mean $^{206}Pb/^{238}U$ ages are not skewed by Pb-loss due to the chemical abrasion pre-treatment procedure, which has been convincingly demonstrated by prior studies to eliminate zircon domains affected by Pb-loss [*Mundil et al.*, 2004; *Mattinson*, 2005]. Moreover, our interpretations do not hinge on deciphering the growth systematics of individual zircon grains.

4.1. Peralkaline Ring Dike

[18] One sample (VC09–02) of a large body of the peralkaline ring dike where it is interpreted to intrude the northern caldera margin [*Lipman and Reed*, 1989] was analyzed (Figure 2a). Four concordant fractions overlap within uncertainty and yield a weighted mean $^{206}Pb/^{238}U$ age of 25.64 ± 0.08 Ma (MSWD = 0.14).

4.2. Amalia Tuff

[19] A sample of the Amalia Tuff was collected from inside the northern part of the caldera (AT09–01;

Table 1. U-Pb Data for Rocks of the Latir Volcanic Field and Questa Caldera[a]

ID (n)	Concentration (ppm)										Ages[d] (Ma)					Total Common Pb (pg)
	U	Pb[b]	Th/U	$^{206}Pb/^{204}Pb$[c]	$^{206}Pb/^{238}U$[d]	Error (%)	$^{207}Pb/^{235}U$[d]	Error (%)	$^{207}Pb/^{206}Pb$[d]	Error (%)	$^{206}Pb/^{238}U$	Error (Ma)	$^{207}Pb/^{235}U$	$^{207}Pb/^{206}Pb$	Correlation Coefficient	
AT09–01 Amalia Tuff (Th/U = 3.8[e]: 0459326, 4073640)[f]																
3 (2)	586.1	2.33	0.206	318.68	0.003964	(.64)	0.02556	(1.0)	0.04678	(.74)	25.50	(0.04)	25.63	37.78	0.677	2.26
10 (5)	1078	4.31	0.234	1619.7	0.003963	(.15)	0.02552	(.31)	0.04670	(.27)	25.50	(0.03)	25.59	34.03	0.519	1.88
11 (6)	575.0	2.31	0.230	1705.3	0.003974	(.13)	0.02561	(.19)	0.04673	(.13)	25.57	(0.11)	25.67	35.49	0.733	1.51
12 (5)	2669	11.8	0.506	1408.5	0.003965	(.44)	0.02547	(.48)	0.04658	(.19)	25.51	(0.16)	25.54	27.71	0.919	8.37
MZQ-09 Rio Hondo Megacrystic (Th/U = 4.0: 0455450, 4049375)																
9 (3)	501.7	1.97	0.804	1487.1	0.003497	(.29)	0.02245	(.05)	0.04656	(.31)	22.59	(0.06)	22.54	17.18	0.693	1.97
10 (4)	818.8	3.15	0.731	1807.7	0.003492	(.27)	0.02238	(.05)	0.04649	(.22)	22.56	(0.06)	22.48	13.61	0.787	2.60
11 (4)	1126	4.27	0.666	2583.6	0.003500	(.19)	0.02242	(.05)	0.04646	(.18)	22.61	(0.04)	22.51	11.60	0.727	2.02
12 (3)	681.2	2.61	0.686	2656.2	0.003516	(.18)	0.02252	(.05)	0.04646	(.18)	22.71	(0.04)	22.62	12.24	0.709	1.96
MZQ-12 Cabresto Lake (Th/U = 4.5: 0454802, 4066600)																
2 (3)	581.3	2.68	0.925	977.51	0.003896	(.57)	0.02490	(.62)	0.04636	(.25)	25.07	(0.14)	24.98	16.17	0.918	5.33
5 (4)	505.8	2.27	0.904	1970.7	0.003905	(.24)	0.02495	(.33)	0.04635	(.22)	25.13	(0.06)	25.03	15.63	0.750	2.21
6 (4)	644.8	2.90	0.900	1374.4	0.003894	(.56)	0.02496	(.60)	0.04649	(.20)	25.06	(0.14)	25.04	23.13	0.943	3.83
7 (3)	486.7	2.09	0.756	1336.7	0.003893	(.31)	0.02487	(.45)	0.04634	(.31)	25.05	(0.08)	24.95	15.26	0.722	3.01
MZQ-13 Cabresto Lake (Th/U = 4.5: 0454797, 4065491)																
17 (2)	422.9	1.88	0.893	647.38	0.003888	(.60)	0.02495	(.72)	0.04655	(.38)	25.01	(0.15)	25.02	25.97	0.850	3.80
19 (3)	716.8	3.16	0.854	1076.2	0.003890	(.37)	0.02491	(.45)	0.04644	(.25)	25.03	(0.09)	24.98	20.48	0.827	3.44
20 (2)	535.9	2.29	0.733	904.58	0.003890	(.44)	0.02483	(.59)	0.04630	(.38)	25.03	(0.11)	24.91	13.52	0.763	3.47
23 (3)	431.0	1.91	0.883	632.72	0.003889	(.62)	0.02482	(.89)	0.04628	(.60)	25.02	(0.15)	24.89	12.51	0.733	3.05
26 (3)	429.1	1.84	0.742	1383.3	0.003889	(.30)	0.02488	(.48)	0.04639	(.36)	25.02	(0.07)	24.95	17.82	0.651	2.29
MZQ-15 Cañada Pinabete Late Metaluminous (Th/U = 5.1: 0450662, 4068102)																
1 (3)	375.1	1.60	0.670	1047.6	0.003935	(.38)	0.02516	(.47)	0.04638	(.27)	25.32	(0.10)	25.24	17.36	0.821	2.55
2 (2)	355.6	1.55	0.769	963.61	0.003936	(.42)	0.02529	(.50)	0.04660	(.26)	25.32	(0.11)	25.36	28.99	0.847	2.96
3 (3)	652.2	2.80	0.713	1839.9	0.003927	(.25)	0.02496	(.65)	0.04610	(.57)	25.27	(0.06)	25.04	2.81	0.487	2.56
5 (5)	392.1	1.73	0.773	1118.2	0.003964	(.36)	0.02530	(.53)	0.04628	(.37)	25.51	(0.09)	25.37	12.33	0.718	2.32

Table 1. (continued)

ID (n)	Concentration (ppm) U	Pb[b]	Th/U	$^{206}Pb/^{204}Pb$[c]	$^{206}Pb/^{238}U$[d]	Error (%)	$^{207}Pb/^{235}U$[d]	Error (%)	$^{207}Pb/^{206}Pb$[d]	Error (%)	Ages[d] (Ma) $^{206}Pb/^{238}U$	Error (Ma)	$^{207}Pb/^{235}U$	$^{207}Pb/^{206}Pb$	Correlation Coefficient	Total Common Pb (pg)
MZQ-19 Rio Hondo (Th/U = 4.0: 0453613, 4055209)																
1 (2)	1132	4.65	0.906	1384.9	0.003531	(.47)	0.02256	(.51)	0.04635	(.19)	22.72	(0.11)	22.66	15.63	0.930	4.64
2 (2)	1014	4.07	0.779	1076.3	0.003534	(.53)	0.02254	(.59)	0.04626	(.25)	22.74	(0.12)	22.63	10.96	0.902	5.18
5 (2)	1082	4.12	0.649	1910.8	0.003536	(.24)	0.02258	(.32)	0.04633	(.21)	22.75	(0.05)	22.68	14.62	0.754	2.84
6 (2)	1076	4.25	0.802	2363.7	0.003532	(.21)	0.02254	(.29)	0.04628	(.19)	22.73	(0.05)	22.63	12.42	0.748	2.69
7 (3)	889.5	3.40	0.679	2858.6	0.003522	(.20)	0.02248	(.31)	0.04628	(.23)	22.67	(0.04)	22.57	12.33	0.667	2.00
MZQ-33 Rio Hondo Granite (Th/U = 6.0: 0453636, 4049302)																
1 (2)	1684	6.33	0.504	2354.8	0.003589	(.28)	0.02290	(.35)	0.04627	(.20)	23.10	(0.06)	22.99	11.78	0.822	5.50
3 (2)	1029	3.90	0.539	1177.0	0.003553	(.52)	0.02269	(.56)	0.04632	(.19)	22.86	(0.12)	22.78	14.07	0.938	4.84
5 (3)	910.1	3.46	0.585	1420.9	0.003583	(.65)	0.02294	(.70)	0.04643	(.26)	23.06	(0.15)	23.03	20.11	0.929	3.15
6 (3)	528.1	1.95	0.494	1099.3	0.003570	(.39)	0.02306	(.47)	0.04685	(.24)	22.98	(0.09)	23.15	41.44	0.857	2.70
7 (3)	766.0	2.87	0.493	1132.6	0.003572	(.60)	0.02288	(.65)	0.04645	(.22)	22.92	(0.08)	22.92	23.32	0.938	4.22
8 (3)	1352	5.26	0.626	1390.3	0.003561	(.36)	0.02283	(.40)	0.04649	(.16)	22.98	(0.14)	22.97	21.03	0.915	5.88
MZQ-40 Rio Hondo Megacrystic (Th/U = 4.0: 0452777, 4046272)																
5 (3)	952.1	3.63	0.625	1653.7	0.003564	(.58)	0.02269	(.65)	0.04618	(.30)	22.93	(0.13)	22.78	7.11	0.892	3.06
6 (2)	707.8	2.71	0.601	1149.4	0.003546	(.58)	0.02256	(.65)	0.04615	(.29)	22.82	(0.13)	22.65	5.55	0.895	4.36
7 (1)	1714	6.50	0.585	1490.2	0.003549	(.48)	0.02267	(.54)	0.04634	(.22)	22.84	(0.11)	22.77	15.08	0.910	4.04
8 (3)	1146	4.42	0.674	1737.4	0.003544	(.47)	0.02270	(.51)	0.04647	(.20)	22.80	(0.11)	22.79	21.85	0.922	3.62
VC09-02 Ring Dike (Th/U = 4.8: 0458237, 4075076)																
11 (2)	562.6	2.27	0.406	575.09	0.003988	(.69)	0.02562	(1.9)	0.04659	(1.7)	25.69	(0.22)	25.77	32.65	0.470	1.12
12 (2)	419.1	1.67	0.386	478.45	0.003979	(.82)	0.02542	(1.1)	0.04633	(.67)	25.66	(0.18)	25.68	28.35	0.787	2.30
19 (3)	541.8	2.19	0.417	853.03	0.003985	(.46)	0.02556	(.52)	0.04652	(.24)	25.64	(0.12)	25.63	24.69	0.887	2.31
20 (2)	216.9	0.872	0.394	447.21	0.003994	(.87)	0.02570	(1.1)	0.04668	(.65)	25.60	(0.21)	25.49	14.89	0.809	1.92

[a]All errors except error in the $^{206}Pb/^{238}U$ age are reported in percent at the 2σ confidence interval. Error in the $^{206}Pb/^{238}U$ age is reported in absolute (Ma) at the 2σ confidence interval.
[b]Radiogenic Pb.
[c]Measured ratio corrected for fractionation only. All Pb isotope ratios were measured using the Daly detector, and are corrected for mass fractionation using 0.15%/amu.
[d]Corrected for fractionation, spike, blank and Th disequilibrium. All common Pb is assumed to be blank.
[e]Th/U assumed for the magma using average whole-rock data from *Johnson et al.* [1989]. All ratios and ages are corrected for Th disequilibrium.
[f]All locations reported as UTM coordinates using NAD 27, section 13S.

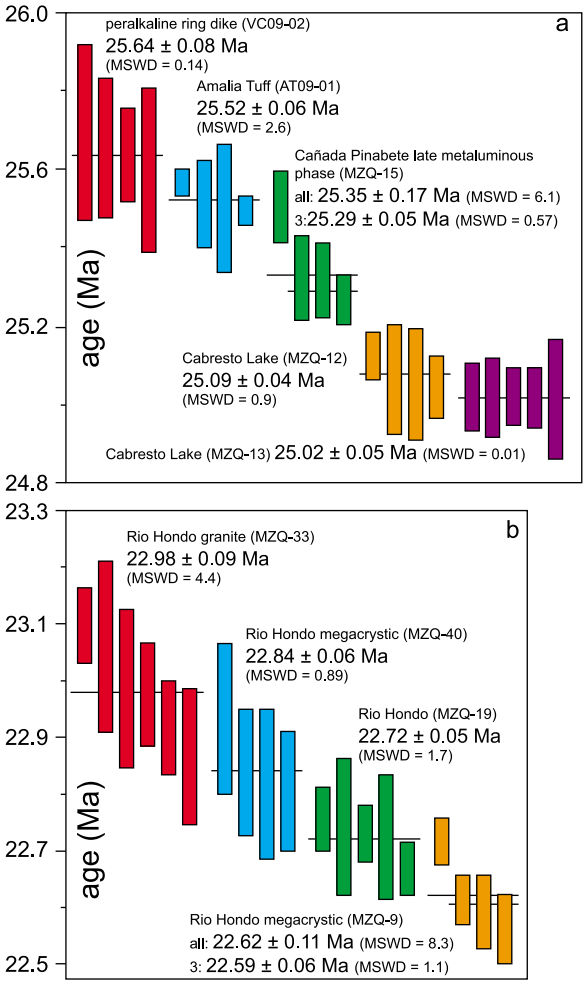

Figure 2. The $^{206}Pb/^{238}U$ ages for zircon from the Latir volcanic field. Data for all samples are concordant within analytical uncertainty, therefore we accept the weighted mean $^{206}Pb/^{238}U$ ages as indicative of the crystallization age. Reported uncertainties do not include uncertainty in decay constants because we are comparing only U/Pb data. We did consider uncertainties in decay constants when discussing these ages with the $^{40}Ar/^{39}Ar$ data reported by Zimmerer and McIntosh (submitted manuscript, 2011) for the same samples. Most samples have fairly simple systematics; however two (MZQ-9 and −15) have one fraction that we interpret to be derived from older parts of the magma system. Samples of the Rio Hondo pluton show a spread in ages typical of incrementally assembled plutons elsewhere [e.g., *Miller et al.*, 2007].

Figure 1b). The sample yielded sparse zircons that give a weighted mean $^{206}Pb/^{238}U$ age of 25.52 ± 0.06 Ma (MSWD = 2.6; Figure 2a). Although some scatter exists in the data for this sample, we find no a priori reason to exclude any analyses, and we take the mean as the best estimate of the age of the tuff sample.

4.3. Cañada Pinabete Pluton

[20] Four fractions from sample MZQ-15 of the late metaluminous phase of the Cañada Pinabete pluton were analyzed (Figure 2). One fraction is distinctly older than the other three, and overlaps within uncertainty with zircon from the peralkaline phase of the Virgin Canyon pluton and the Amalia Tuff. This fraction included 5 of the smallest grains analyzed (in contrast to 2 or 3 grains in the other fractions analyzed); consequently, it may contain a small antecryst component in one or more of the grains. The weighted mean $^{206}Pb/^{238}U$ age of all the fractions is 25.35 ± 0.17 Ma (MSWD = 6.1), and that of the three overlapping fractions is 25.29 ± 0.05 Ma (MSWD = 0.57).

4.4. Cabresto Lake Pluton

[21] Two samples of the Cabresto Lake pluton taken very close to one another (MZQ-12 and MZQ-13) were dated (Figure 1b). Results for the two samples yield overlapping weighted mean ages of 25.09 ± 0.04 Ma (MSWD = 0.9; 4 fractions from MZQ-12) and 25.02 ± 0.05 Ma (MSWD = 0.01; 5 fractions from MZQ-13).

4.5. Rio Hondo Pluton

[22] Four spatially, compositionally and texturally distinct samples (MZQ-9, MZQ-19, MZQ-33, and MZQ-40) of the Rio Hondo pluton were analyzed (Figure 1b). The structurally highest sample (MZQ-33) is high-silica granite collected from near the interpreted roof [*Lipman*, 1988; *Czamanske et al.*, 1990]. Samples MZQ-19, MZQ-9, and MZQ-40 are quartz monzonite with the latter two hosting rapakivi K-feldspar megacrysts. Most samples yield ages that scatter beyond analytical uncertainty. One sample is characterized by three overlapping fractions and a single outlier (MZQ-9; Figure 2b). The weighted mean $^{206}Pb/^{238}U$ for all the fractions from this sample is 22.62 ± 0.11 Ma, and that of the three overlapping fractions is 22.59 ± 0.03 Ma. Taken together, the Rio Hondo zircons yield a spectrum of $^{206}Pb/^{238}U$ ages from 23.10 to 22.56 Ma and data from samples overlap (Figure 2b). However, taken individually, each sample tends to cluster relative to the entire data array, and there is a distinction between the age of the oldest roof granite (22.98 ± 0.09 Ma) and the youngest megacrystic quartz monzonite (22.59 ± 0.03 Ma). Although the roof granite

intrudes Precambrian wall rock there is no evidence in the zircon systematics to suggest the assimilation of any Precambrian, xenocrystic zircon.

5. Discussion

5.1. Crystallization and Cooling of Questa Caldera Intrusive Rocks

[23] We take the weighted mean $^{206}Pb/^{238}U$ ages shown in Figure 2 as crystallization ages of the samples. Two samples (the late metaluminous phase of the Cañada Pinabete pluton and the youngest sample of the megacrystic Rio Hondo pluton) are interpreted to have minor inheritance of zircon from older parts of the intrusive system as described in other plutons [*Miller et al.*, 2007]. For both of these, the younger cluster of ages is taken as the crystallization age (25.29 Ma and 22.59 Ma, respectively).

[24] Zircon separates were obtained from the identical samples that Zimmerer and McIntosh (submitted manuscript, 2011) dated using $^{40}Ar/^{39}Ar$. Of the samples dated in this study, they obtained reliable biotite dates for five samples, including the late metaluminous Cañada Pinabete (MZQ-15), and two samples each from the Cabresto Lake (MZQ-12 and −13), and Rio Hondo (MZQ-9 and −19) plutons (Table 1). The intracaldera samples yield biotite dates that overlap within uncertainty with the U/Pb zircon ages; however, biotite dates for the Rio Hondo pluton are younger than the zircon ages by nearly 1 Ma, consistent with more protracted cooling. Using geochemical data from *Johnson et al.* [1989], the zircon saturation temperature is calculated to be approximately 800°C for the Virgin Canyon and Cabresto Lake plutons and approximately 725°C for the Rio Hondo pluton [*Watson and Harrison*, 1983]. For all samples, therefore, cooling between 700 and 800°C to 280–345°C (estimated biotite closure temperatures [*Harrison et al.*, 1985]) occurred in less than a million years, consistent with intrusion at shallow crustal depths (<5 km) [*Lipman*, 1988]. Consequently, we interpret the crystallization age of each sample to be representative of the intrusion age.

[25] The ages determined in this study support previous interpretations of magmatism beginning with the northern plutons and migrating south [*Lipman et al.*, 1986; *Czamanske et al.*, 1990]. The new data show that the peralkaline ring dike associated with the Virgin Canyon pluton in the north is the same age within uncertainty as the Amalia Tuff. The data also demonstrate that the Cabresto Lake pluton, located near the mapped center of the caldera, was resurgent into the caldera approximately 500 ka after caldera formation. Finally, the data show that the Rio Hondo pluton (to the south and outside of the caldera) formed over at least 400 ka, beginning approximately 2.5 Ma after ignimbrite eruption.

5.2. Plutonic-Volcanic Rock Pairs at Latir

[26] The zircon U/Pb ages of the peralkaline ring dike (25.64 ± 0.08 Ma) and Amalia Tuff (25.52 ± 0.06 Ma) overlap within uncertainty, and are slightly older than the sanidine $^{40}Ar/^{39}Ar$ age (25.39 ± 0.04 Ma) of the Amalia Tuff reported by Zimmerer and McIntosh (submitted manuscript, 2011). If uncertainties in decay constants are considered for both U and K, the ages overlap within uncertainty. Alternatively, this small difference could reflect pre-eruptive zircon growth [*Simon et al.*, 2008]. Independent of the origin of the discrepancy between U-Pb and Ar ages, overlap of U-Pb dates suggests that the peralkaline ring dike is the unerupted equivalent of the Amalia Tuff, consistent with the early correlation of the units made on the basis of petrographic and geochemical similarity [*Lipman*, 1988; *Johnson et al.*, 1989].

[27] The zircon data suggest that the late metaluminous granite of the Cañada Pinabete pluton is younger than the ring dike and the tuff. This corroborates field relations [*Lipman*, 1988] that indicate the dated metaluminous phase was late relative to the peralkaline and early metaluminous phases. The occurrence of a single zircon fraction from the late metaluminous phase that is identical in age to the zircons from the peralkaline phase and the tuff (Figure 2a) is consistent with incorporation of antecrystic zircon from early phases of the magma system into later phases [*Miller et al.*, 2007].

[28] No precaldera plutons that could be correlative to precaldera volcanic rocks were identified in this, or earlier studies. However, post-caldera intrusion of the Rio Hondo pluton (~23–22.5 Ma) is coincident with eruption of the Brushy Mountain Andesite (22.69 Ma groundmass concentrate $^{40}Ar/^{39}Ar$). Petrographically, the olivine-bearing andesite [*Thompson et al.*, 1986] is unlike any rocks preserved in the Rio Hondo pluton. Additional data are necessary to evaluate if the dacite lavas that overlie the andesite at Brushy and Timber Mountains might be directly related to the youngest phases of the Rio Hondo pluton.

5.3. Top-Down Pluton Construction and the Origin of Zoned Plutons

[29] Within the Cañada Pinabete pluton, field, paleomagnetic, and petrologic studies suggest the structurally highest early metaluminous phase intruded before the structurally deepest late metaluminous phase, and that intrusion of both of these postdates intrusion of the peralkaline phase that is correlative with the Amalia Tuff [*Hagstrum and Lipman*, 1986; *Johnson et al.*, 1989; *Lipman*, 1988]. Geochronologic data presented here corroborate the observation that the late metaluminous phase is younger than the peralkaline phase and the tuff. The new age data, combined with the relative stratigraphic relationships, demonstrate that this unit accumulated as incrementally intruded bodies from the top downward to the exposed bottom.

[30] Top-down construction of the Rio Hondo pluton is also supported by the zircon geochronology. Zircon U-Pb ages for the structurally highest granite against the mapped roof of the pluton yields the oldest age (22.98 ± 0.09 Ma), and the structurally lower quartz monzonites yield younger ages (22.84 ± 0.06; 22.72 ± 0.05; 22.59 ± 0.06 Ma). The older age of the roof granite cannot be the result of the presence of Precambrian zircon xenocrysts because even a small inherited Precambrian component would result in significant age discordance in such a young sample.

[31] These two examples of apparent top-down pluton assembly from Questa add to a growing number of examples that suggest that downward stacking of intrusions may be a common assembly sequence. High-precision geochronology and field relations suggest that the Tuolumne [*Coleman et al.*, 2008] and Whitney [*Hirt*, 2007] intrusive suites of the Sierra Nevada batholith, the Trachyte Mesa laccolith of the Henry Mountains [*Morgan et al.*, 2008], the Torres Del Paine complex [*Michel et al.*, 2008], and other South American Cordilleran plutons [*Cruden et al.*, 2005] are downward-stacked sill (or laccolith)-type intrusions. Recent experimental studies predict downward stacking as a dominant mode of incremental pluton assembly [*Kavanagh et al.*, 2006; *Menand*, 2008, 2011]. These experiments demonstrate that magma rising along dikes can stall at rheological boundaries. Rising magma then spreads laterally at the boundary, and sill or laccolith formation is likely to occur.

[32] In the Questa caldera, it is unclear why any of the initial intrusions spread laterally where they did. Tops of plutons in this area are typically located within Precambrian rocks or the base of the Tertiary volcanic pile [*Lipman*, 1988]. However, the bases of the plutons are not exposed. Regardless, once the initial intrusion is emplaced, it likely acted as a rheological barrier, trapping later pulses below. The rheological barriers may have formed either because the initial intrusions crystallized quickly, becoming a cohesive unit that resisted fracturing, or because the sheet contained melt when the next pulse of magma intruded [*Bartley et al.*, 2005; *Coleman et al.*, 2008]. If significant melt was still present, brittle deformation necessary for dike propagation is unlikely to have occurred when the next magma pulse intruded, thus trapping later pulses below earlier ones [*Bacon et al.*, 1980; *Wiebe and Collins*, 1998].

[33] The top-down sequence in the Rio Hondo pluton is particularly significant because the pluton is normally zoned with a silicic cap above more mafic quartz monzonite. Here [*Johnson et al.*, 1989] and elsewhere [*Hildreth*, 1981, 2004], this progression has been interpreted to reflect accumulation of a dominantly liquid silicic cap above a more mafic, crystal-rich body. Alternatively, the silicic cap composition could reflect assimilation or other significant interaction with the country rocks. However, there is no evidence for upper crustal interaction in isotopic [*Johnson et al.*, 1990] or zircon systematics of the roof granite, yet it is distinctly older than the parts of the pluton that should have crystallized first according to the in situ differentiation hypothesis. The zircon saturation temperature of the granite (720°–730°C) is comparable to (or perhaps, lower than) that of the quartz monzonite (750°–760°C). Consequently, if the rocks were all part of the same magma chamber, there is no reason why the granite should have initiated zircon crystallization before the quartz monzonite unless it was cooling and crystallizing against the roof – in which case, it cannot have been a dominantly liquid silicic cap sitting above a crystal-liquid residue.

[34] Because the roof granite is older than the deeper "less fractionated" parts of the Rio Hondo pluton, and because there is no evidence for assimilation, we suggest that the normal zoning of the pluton occurred independently of processes that occurred at the level of emplacement. Although some modification of the magmas may have occurred in the shallow crust, we propose that the temporal progression of magmas that accumulated to form the Rio Hondo pluton is dominated by the temporal evolution of the magmas derived from the source, which is likely to be the lower crust [*Johnson and Lipman*, 1988; *Johnson et al.*, 1990]. The same

process may be responsible for the formation of other zoned plutons.

5.4. Pluton Accumulation Rates for the Rio Hondo Pluton

[35] The well-determined geochronology of the Rio Hondo pluton provides an opportunity to examine pluton-filling rates for the exposed volume. The U-Pb zircon geochronology suggests that the exposed portion of the Rio Hondo pluton took at least 400 ka to accumulate. Whether the Rio Hondo pluton exposures provide a complete view of the entire body is debatable. The roof of the pluton is exposed at low-angle contacts between plutonic and basement rocks along ridge crests [*Lipman*, 1988]. At low elevations, the Rio Hondo pluton contains high concentrations of mafic enclaves that are interpreted in other plutons to indicate a level near the pluton floor [*Wiebe et al.*, 1997; *Bachl et al.*, 2001]. However, geophysical data suggest that a significantly thicker body of granitic rock underlies a large area under the Latir volcanic field [*Cordell et al.*, 1985]. It is unclear if any of this body is the same age or directly genetically related to the Rio Hondo pluton. Consequently, we take a conservative approach and limit our estimate of the filling rate to the dated, observable volume of the Rio Hondo pluton, and consider extrapolating to the entire geophysically imaged body separately.

[36] The surface exposure of the Rio Hondo pluton implied by the minimum outcrop area is 90 km^2 and the exposed vertical relief of samples collected for geochronology is 1.2 km. These numbers yield an aspect ratio of approximately 8:1, comparable to other pluton aspect ratios where better estimates of complete thickness can be made [*Cruden and McCaffrey*, 2001; *Bachmann and Bergantz*, 2008a]. Assuming that the dated volume of the Rio Hondo can be approximated as a cylinder (given documentation of a flat roof and steep margins [*Lipman*, 1988]) and using a filling time of 400 ka yields an integrated filling rate of 0.0003 km^3 a^{-1}, although actual magma flux at any time would likely be higher or lower than the integrated, long-term value. Estimated filling rates for plutons elsewhere with precise geochronologic control yield similar time-averaged rates, ranging from 0.0002 to 0.0008 km^3 a^{-1} [*Coleman et al.*, 2004; *Matzel et al.*, 2006; *Davis et al.*, 2011]. These rates are at the low end of the range of rates suggested by *Petford et al.* [2000] for pluton accumulation, and several orders of magnitude slower than the minimum rates calculated by *Annen* [2009] to support the production of large volumes of eruptible magma. The slow accumulation rate for the Rio Hondo pluton is consistent with the observation that there are no known ignimbrites of the same age as the dated portion of pluton.

5.5. Pluton Accumulation Rates at Latir

[37] Gravity lows are commonly found in the subsurface beneath caldera systems [e.g., *Davy and Caldwell*, 1998; *Marti et al.*, 2008], and whereas some interpretations suggest they represent the plutonic rock from which the ignimbrite was fractionated [*Lipman*, 2007], others suggest these anomalies reflect the presence of postcaldera intrusions [*Steck et al.*, 1998]. Geophysical surveys of the Latir volcanic field suggest that it is underlain by a large pluton or set of plutons with an estimated volume of 4500 km^3 [*Cordell et al.*, 1985; *Long*, 1985; *Lipman*, 1988]. The most recent models for the formation of the plutons beneath the Latir volcanic field demand an episodic intrusive history, but also suggest that the bulk of the intrusive rocks had a short (less than 500 ka) magmatic history [*Lipman*, 1988]. Furthermore, these models assume that the bulk of the unexposed plutonic rocks intruded coincidentally with eruption of the Amalia Tuff [*Lipman*, 2007], and that the plutons dated in this study represent small cupolas of that large body [*Lipman*, 1988].

[38] The new U-Pb and $^{40}Ar/^{39}Ar$ data presented here and by Zimmerer and McIntosh (submitted manuscript, 2011) offer reason to question the hypothesis that the unexposed plutonic rocks beneath the Latir volcanic field are the unerupted crystal + liquid residue of the Amalia Tuff. Most significantly, the Rio Hondo pluton is 2.5 Ma younger than the tuff, and all of the plutons for which there are U-Pb and biotite $^{40}Ar/^{39}Ar$ data indicate cooling below biotite closure within 1 Ma of zircon saturation. It seems unlikely that a large magma body only a few kilometers below the level of exposure could remain molten (and above zircon saturation temperatures) for millions of years then reach zircon saturation temperatures and crystallize almost instantaneously 2.5 Ma later when it rose as a cupola.

[39] Alternatively, extrapolation of the time-averaged pluton accumulation rate estimated during assembly of the exposed portion of the Rio Hondo pluton throughout the 9.5 Ma history of the Latir field (~28.5 to 19 Ma) (Zimmerer and McIntosh, submitted manuscript, 2011) predicts a total intrusive volume of approximately 2900 km^3. Accumulating the total pluton volume of 4500 km^3 inferred

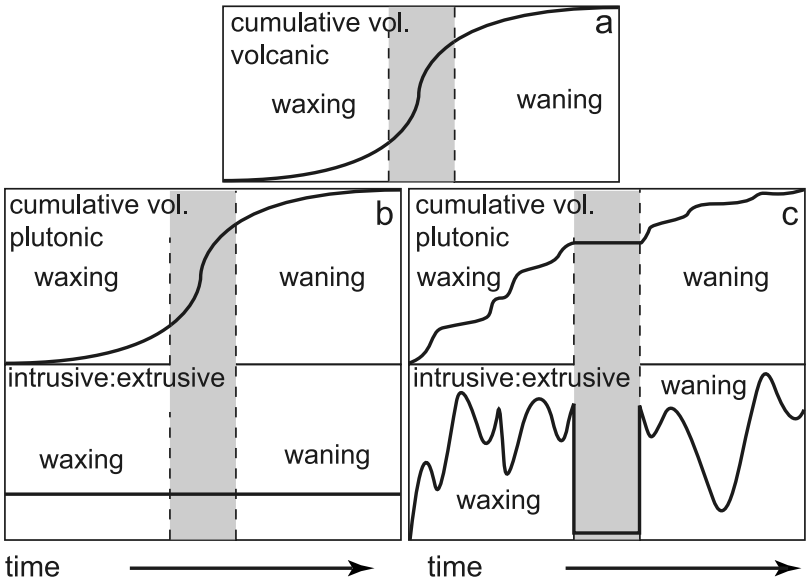

Figure 3. (a) Simplified representation of the volcanic cycle proposed for silicic ignimbrite magmatism and (b) traditional and (c) proposed models for plutonic and volcanic rock relationships during this magmatism. Waxing, ignimbrite (shaded) and waning stages of magmatism after *Lipman* [2007]. The volcanic record (Figure 3a) is well documented [e.g., *Lipman*, 2007], and is the same for both intrusive rock scenarios. Accumulation of volcanic rocks spikes during the ignimbrite stage, and represents the same interval on all three diagrams. No scale on either the horizontal or vertical axes is implied, only that at the onset of magmatism the cumulative volume of both volcanic and plutonic rocks is zero, and by the end, the entire volume of each is present. Likewise, no specific intrusive:extrusive ratio is implied. The traditional model (Figure 3b) predicts accumulation of plutonic rocks proportional to the erupted volcanic rocks, and a relatively constant intrusive:extrusive rock ratio. Alternatively, in Figure 3c, data from Questa suggest there is essentially nothing in the plutonic record from the ignimbrite stage, and we propose that the high flux of magma necessary to generate an ignimbrite results in near total evacuation of the magma. Furthermore, the intrusive:extrusive ratio is likely to be highly variable for individual events. The model also requires that the intrusive:extrusive ratio for the waxing and waning stages is higher, on average than the traditional model.

from the geophysical anomaly requires a long-term average pluton accumulation rate of ~0.0005 km^3 a^{-1} over the age range of the Latir field – a rate that is within uncertainty of the estimate for accumulation rate of the Rio Hondo pluton, and well within published estimates for plutons from elsewhere. Although extrapolation of the time averaged flux from a short time and a small volume of plutonic rocks to the entire history and volume for the Latir field is debatable, it is remarkable (given all the assumptions) that the estimates are the same order of magnitude. If the assumptions are all valid, the somewhat slower than average accumulation rate during assembly of the Rio Hondo pluton might be expected because it formed during the waning stage of magmatism in the Latir field.

5.6. What Is the Link Between Plutonic and Volcanic Rocks?

[40] Presently, it is widely accepted that there is a range of high intrusive:extrusive rock ratios typical of magma centers (Figure 3), and that plutonic rocks represent crystal and liquid residua left after differentiation and formation of an eruptible, dominantly liquid cap on a shallow magma chamber [e.g., *Smith*, 1979; *Hildreth*, 2004; *White et al.*, 2006; *de Silva et al.*, 2007]. However, we believe the data from the Latir volcanic field offer a different possibility.

[41] The first key observation from the Latir field is that the bulk of the plutonic rocks are younger than the volcanic rocks, precluding the possibility that differentiation of the plutons produced the ignimbrite. The second observation is that accumulation of the entire volume of plutonic rocks inferred to be preserved under the volcanic field could have been accomplished over the lifetime of the field at a time-averaged rate comparable to the rate measured for the Rio Hondo pluton and plutons from other environments. Thus, there is no reason to call on the existence of a rapidly accumulated pluton for which there is no direct evidence here or elsewhere. The last key observation is that chemical zoning in the Rio Hondo pluton could not have formed at the

present level of exposure. Even though fractional crystallization models can successfully reproduce the observed variation [*Johnson et al.*, 1989], the geochronologic data preclude this possibility. Consequently, there is no requirement for a large shallow magma body to generate the observed chemical variability.

[42] We suggest that the intrusive rocks beneath the Latir volcanic field represent a cumulative volume assembled over the history of the field and that the only plutonic remnant of the ignimbrite magma, exposed or buried, is the small-volume ring dike of composition comparable to the Amalia Tuff (Figure 3c). This proposal is consistent with modeling experiments that suggest that total magma chamber evacuation can occur during ignimbrite eruptions [*Roche and Druitt*, 2001; *Geyer et al.*, 2006]. It is also consistent with the observation that the magma responsible for eruption of the peralkaline Amalia Tuff cannot be related to the exposed penecontemporaneous plutons by any simple fractionation model [*Johnson et al.*, 1989]. Because there is no direct evidence for a large coeval pluton, we favor the interpretation that the tuff was derived through a distinct melting event in the lower crust [*Johnson et al.*, 1989].

[43] In this interpretation, the relatively low flux of magma that characterizes the waxing and waning stages of magmatism during development of silicic ignimbrite systems, here and elsewhere, favors trapping of magma in the crust. It is possible that during an extremely low flux event, the entire magma may get trapped as part of an incrementally growing pluton. In contrast, the extreme fluxes implied by ignimbrite eruption result in nearly complete eruption of the rising magma. The intrusive:extrusive rock ratio may vary between near infinity and near zero (Figure 3c). Importantly, if the ignimbrite eruption dominates the volume of rock preserved in the volcanic record, but is essentially absent from the plutonic record, the existing estimates of the intrusive:extrusive rock ratio [*White et al.*, 2006] are skewed low for the dominant instantaneous ratio, but may be more accurate for the entire lifetime of an ignimbrite center. Arguably, the instantaneous ratio is the most significant because it is directly tied to the genetic link between plutonic and volcanic rocks.

[44] A high intrusive:extrusive rock ratio is required if ignimbrite composition is controlled by shallow crustal fractionation [*Hildreth*, 2004]. However, if large volcanic eruptions are not supported by proportionately large pluton volumes, then the bulk geochemistry of ignimbrites, and the origin of zonation in ignimbrites, is not the result of shallow crustal processes [*Simon et al.*, 2007]. *Clemens et al.* [2009] recently asserted as much, suggesting that the geochemistry of igneous rocks is dominated by a signal from their source in the lower crust. Although it is possible to model the geochemical variation observed in Latir volcanic [*Johnson and Lipman*, 1988] and plutonic [*Johnson et al.*, 1989] rocks through shallow crustal fractional crystallization, the geochronologic data for the Rio Hondo pluton offer evidence to suggest that the same geochemical variation can be generated without it. Consequently, the chemical variation observed in zoned ignimbrites could form during periods of high magma flux with little, or no, shallow crustal residence time as suggested for the Bishop Tuff [*Simon and Reid*, 2005; *Simon et al.*, 2007].

6. Conclusions

[45] New zircon geochronologic data for plutonic rocks exposed in and around the Questa caldera of the Latir volcanic field confirm that the only exposed plutonic rock coeval with the Amalia Tuff is the discontinuous dike preserved along the northern ring fracture of the caldera. Intracaldera plutons all appear to be resurgent, having intruded and cooled quickly within 500 ka of ignimbrite eruption. The Rio Hondo pluton crops out entirely outside the mapped caldera, is the largest pluton exposed, and was assembled incrementally 2.5 Ma after caldera eruption.

[46] Assembly of the exposed portion of the Rio Hondo pluton was far too protracted to have supported a large eruption, which is corroborated by the lack of any contemporaneous ignimbrite in the volcanic rock record. More importantly, the geochronologic data contradict the interpretation that zoning in the pluton developed in situ. Instead, the zoning is interpreted to reflect a change in the composition of the magma arriving at the level of emplacement from the source. Because internal pluton zoning has been correlated with zoning in ignimbrites, we suggest that zoning in ignimbrites could also reflect changes in source magmas, and need not result from shallow fractionation. Extrapolation of the magma accumulation rate for the Rio Hondo over the lifetime of the Latir volcanic field suggests that the volume of unexposed plutonic rocks inferred from geophysical data could have accumulated without the formation of a large pluton coincident with ignimbrite formation.

[47] There is no direct evidence linking the bulk of the inferred plutonic rocks at Latir with the eruption of the Amalia Tuff. Therefore, we suggest that the data from Latir are consistent with a new model of plutonic-volcanic rock connection that accumulates the bulk of the plutonic rocks during periods of low magma flux during the waxing and waning stages of caldera formation. Whereas low magma flux during the waxing and waning stages may favor trapping magmas as plutons, the high magma flux necessary to form large ignimbrites favors near total evacuation of the magmas. According to this interpretation, the plutonic-volcanic rock connection does not require that plutons are residual crystals and liquid remaining after a fraction of the liquid is removed. Instead, plutonic rocks represent texturally modified equivalents of the magmas that erupt during low flux periods.

Acknowledgments

[48] Tappa and Mills received funding from the UNC Martin fund. Tappa also received funding from the USGS through Ren Thompson in support of field research. Mills received funding from Sigma Xi, and Samperton received funding from the Dunlevie Undergraduate Honors Research Fund, UNC Honors Office. Field work could not have been conducted without the help of collaborator Matt Zimmerer. Peter Lipman and Allen Glazner reviewed early versions of this manuscript. Journal reviews by Shan de Silva, Mark Schmitz, and an anonymous reviewer significantly improved the quality and clarity of the manuscript. The ideas in this manuscript benefited tremendously from discussions with Peter Lipman, Matt Zimmerer, Bill McIntosh, Allen Glazner, John Bartley, Jesse Davis and Jan Tympel, though they may individually agree with few of the discussion points, interpretations or conclusions. Jesse Davis and John Gracely helped tremendously with the laboratory work.

References

Annen, C. (2009), From plutons to magma chambers: Thermal constraints on the accumulation of eruptible silicic magma in the upper crust, *Earth Planet. Sci. Lett.*, *284*, 409–416, doi:10.1016/j.epsl.2009.05.006.

Bachl, C. A., C. F. Miller, J. S. Miller, and J. E. Faulds (2001), Construction of a pluton: Evidence from an exposed cross section of the Searchlight Pluton, Eldorado Mountains, Nevada, *Geol. Soc. Am. Bull.*, *113*(9), 1213–1228, doi:10.1130/0016-7606(2001)113<1213:COAPEF>2.0.CO;2.

Bachmann, O., and G. W. Bergantz (2004), On the origin of crystal-pore rhyolites extracted from batholithic crystal mushes, *J. Petrol.*, *45*(8), 1565–1582, doi:10.1093/petrology/egh019.

Bachmann, O., and G. W. Bergantz (2008a), The magma reservoirs that feed supereruptions, *Elements*, *4*(1), 17–21, doi:10.2113/GSELEMENTS.4.1.17.

Bachmann, O., and G. W. Bergantz (2008b), Rhyolites and their source mushes across tectonic settings, *J. Petrol.*, *49*(12), 2277–2285, doi:10.1093/petrology/egn068.

Bachmann, O., C. F. Miller, and S. L. de Silva (2007), The volcanic-plutonic connection as a stage for understanding crustal magmatism, *J. Volcanol. Geotherm. Res.*, *167*(1–4), 1–23, doi:10.1016/j.jvolgeores.2007.08.002.

Bacon, C. R., W. A. Duffield, and K. Nakamura (1980), Distribution of Quaternary rhyolite domes of the Coso Range, California: Implications for extent of the geothermal anomaly, *J. Geophys. Res.*, *85*(B5), 2425–2433, doi:10.1029/JB085iB05p02425.

Bartley, J. M., D. S. Coleman, and A. F. Glazner (2005), Incremental pluton emplacement by magmatic crack-seal, *Trans. R. Soc. Edinburgh*, *97*(4), 383–396.

Chapin, C. E. (1979), Evolution of the Rio Grande Rift: A summary, in *Rio Grande Rift; Tectonics and Magmatism*, edited by R. E. Riecker, pp. 1–5, AGU, Washington, D. C.

Clemens, J. D., P. A. Helps, and G. Stevens (2009), Chemical structure in granitic magmas–a signal from the source?, *Trans. R. Soc. Edinburgh*, *100*, 159–172, doi:10.1017/S1755691009016053.

Coleman, D. S., W. Gray, and A. F. Glazner (2004), Rethinking the emplacement and evolution of zoned plutons: Geochronologic evidence for incremental assembly of the Tuolumne Intrusive Suite, *Calif. Geol.*, *32*(5), 433–436.

Coleman, D. S., J. W. Davis, J. M. Bartley, and A. F. Glazner (2008), Downward stacking laccoliths, paper presented at LASI III Conference, Univ. di Pisa, Elba Island, Italy.

Cordell, L., C. L. Long, and D. W. Jones (1985), Geophysical expression of the batholith beneath Questa Caldera, New Mexico, *J. Geophys. Res.*, *90*(B13), 11,263–11,269, doi:10.1029/JB090iB13p11263.

Crowley, J. L., B. Schoene, and S. A. Bowring (2007), U-Pb dating of zircon in the Bishop Tuff at the millennial scale, *Geology*, *35*, 1123–1126, doi:10.1130/G24017A.1.

Cruden, A. R., and K. J. W. McCaffrey (2001), Growth of plutons by floor subsidence; implications for rates of emplacement, intrusion spacing and melt-extraction mechanisms, *Phys. Chem. Earth*, *26*(4–5), 303–315.

Cruden, A. R., J. Grocott, K. J. W. McCaffrey, and D. D. Davis (2005), Timescales of incremental pluton growth: Theory and a field-based test, *Geol. Soc. Am. Abstr. Programs*, *37*(7), 131.

Czamanske, G. K., K. A. Foland, F. A. Kubacher, and J. C. Allen (1990), The $^{40}Ar/^{39}Ar$ chronology of caldera formation, intrusive activity and Mo-ore deposition near Questa, in *Guidebook—New Mexico Geological Society*, edited by P. W. et al., pp. 355–358, N. M. Geol. Soc., Socorro.

Davis, J. W., D. S. Coleman, J. T. Gracely, R. Gaschnig, and M. Stearns (2011), Magma accumulation rates and thermal histories of plutons of the Sierra Nevada batholith, CA, *Contrib. Mineral. Petrol.*, doi:10.1007/s00410-011-0683-7, in press.

Davy, B. W., and T. G. Caldwell (1998), Gravity, magnetic, and seismic surveys of the caldera complex, Lake Taupo, North Isand, New Zealand, *J. Volcanol. Geotherm. Res.*, *81*(1–2), 69–89, doi:10.1016/S0377-0273(97)00074-7.

de Silva, S. L., and W. D. Gosnold (2007), Episodic construction of batholiths: Insights from the spatiotemporal development of an ignimbrite flare-up, *J. Volcanol. Geotherm. Res.*, *167*(1–4), 320–335, doi:10.1016/j.jvolgeores.2007.07.015.

de Silva, S. L., O. Bachmann, C. F. Miller, T. Yoshida, and K. Knesel (2007), Preface to large silicic magmatic systems, *J. Volcanol. Geotherm. Res.*, *167*, vii–ix, doi:10.1016/j.jvolgeores.2007.10.001.

Eichelberger, J. C., P. E. Izbekov, and B. L. Browne (2006), Bulk chemical trends at arc volcanoes are not liquid lines of descent, *Lithos*, *87*(1–2), 135–154, doi:10.1016/j.lithos.2005.05.006.

Geyer, A., A. Folch, and J. Marti (2006), Relationship between caldera collapse and magma chamber withdrawal: An experimental approach, *J. Volcanol. Geotherm. Res.*, *157*(4), 375–386, doi:10.1016/j.jvolgeores.2006.05.001.

Glazner, A. F., J. M. Bartley, D. S. Coleman, W. Gray, and R. Z. Taylor (2004), Are plutons assembled over millions of years by amalgamation from small magma chambers?, *GSA Today*, *14*(4–5), 4–11, doi:10.1130/1052-5173(2004)014<0004:APAOMO>2.0.CO;2.

Glazner, A. F., D. S. Coleman, and J. M. Bartley (2008), The tenuous connection between high-silica rhyolites and granodiorite plutons, *Geology*, *36*(2), 183–186, doi:10.1130/G24496A.1.

Hagstrum, J. T., and P. W. Lipman (1986), Paleomagnetism of the structurally deformed Latir volcanic field, northern New Mexico: Relations to formation of the Questa caldera and development of the Rio Grande rift, *J. Geophys. Res.*, *91*(B7), 7383–7402, doi:10.1029/JB091iB07p07383.

Harrison, T. M., I. Duncan, and I. McDougall (1985), Diffusion of ^{40}Ar in biotite: Temperature, pressure and compositional effects, *Geochim. Cosmochim. Acta*, *49*(11), 2461–2468, doi:10.1016/0016-7037(85)90246-7.

Hildreth, W. (1981), Gradients in silicic magma chambers: Implications for lithospheric magmatism, *J. Geophys. Res.*, *86*(B11), 10,153–10,192, doi:10.1029/JB086iB11p10153.

Hildreth, W. (2004), Volcanological perspectives on Long Valley, Mammoth Mountain, and Mono Craters: Several contiguous but discrete systems, *J. Volcanol. Geotherm. Res.*, *136*(3–4), 169–198, doi:10.1016/j.jvolgeores.2004.05.019.

Hirt, W. H. (2007). Petrology of the Mount Whitney Intrusive Suite, eastern Sierra Nevada, California: Implications for the emplacement and differentiation of composite felsic intrusions, *Geol. Soc. Am. Bull.*, *119*(9–10), 1185–1200.

Johnson, C. M., and P. W. Lipman (1988), Origin of metaluminous and alkaline volcanic rocks of the Latir volcanic field, northern Rio Grande Rift, New Mexico, *Contrib. Mineral. Petrol.*, *100*(1), 107–128, doi:10.1007/BF00399442.

Johnson, C. M., G. K. Czamanske, and P. W. Lipman (1989), Geochemistry of intrusive rocks associated with the Latir volcanic field, New Mexico, and contrasts between evolution of plutonic and volcanic rocks, *Contrib. Mineral. Petrol.*, *103*(1), 90–109, doi:10.1007/BF00371367.

Johnson, C. M., P. W. Lipman, and G. K. Czamanske (1990), H, O, Sr, Nd, and Pb isotope geochemistry of the Latir volcanic field and cogenetic intrusions, New Mexico, and relations between evolution of a continental magmatic center and modifications of the lithosphere, *Contrib. Mineral. Petrol.*, *104*(1), 99–124, doi:10.1007/BF00310649.

Kavanagh, J. L., T. Menand, and R. S. J. Sparks (2006), An experimental investigation of sill formation and propagation in layered elastic media, *Earth Planet. Sci. Lett.*, *245*(3–4), 799–813, doi:10.1016/j.epsl.2006.03.025.

Krogh, T. E. (1973), A low-contamination method for hydrothermal decomposition of zircon and extraction of U and Pb for isotopic age determinations, *Geochim. Cosmochim. Acta*, *37*(3), 485–494, doi:10.1016/0016-7037(73)90213-5.

Lipman, P. W. (1984), The roots of ash flow calderas in western North America: Windows into the tops of granitic batholiths, *J. Geophys. Res.*, *89*(B10), 8801–8841, doi:10.1029/JB089iB10p08801.

Lipman, P. W. (1988), Evolution of silicic magma in the upper crust: The mid-Tertiary Latir volcanic field and its cogenetic granitic batholith, northern New Mexico, U.S.A., *Trans. R. Soc. Edinburgh*, *79*(2–3), 265–288.

Lipman, P. W. (2000), The central San Juan caldera cluster: Regional volcanic framework, in *Ancient Lake Creede: Its Volcano-Tectonic Setting, History of Sedimentation, and Relation of Mineralization in the Creede Mining District*, edited by P. M. Bethke and R. L. Hay, *Spec. Pap. Geol. Soc. Am.*, *346*, 9–69.

Lipman, P. W. (2007), Incremental assembly and prolonged consolidation of Cordilleran magma chambers: Evidence from the Southern Rocky Mountain volcanic field, *Geosphere*, *3*(1), 42–70, doi:10.1130/GES00061.1.

Lipman, P. W., and J. C. Reed Jr. (1989), Geologic map of the Latir volcanic field and adjacent areas, northern New Mexico, scale 1:48,000, *U.S. Geol. Surv. Misc. Map, I-1907*.

Lipman, P. W., H. H. Mehnert, and C. W. Naeser (1986), Evolution of the Latir volcanic field, northern New Mexico, and its relation to the Rio Grande Rift, as indicated by potassium-argon and fission track dating, *J. Geophys. Res.*, *91*(B6), 6329–6345, doi:10.1029/JB091iB06p06329.

Long, C. L. (1985), Regional audiomagnetotelluric study of the Questa Caldera, New Mexico, *J. Geophys. Res.*, *90*(B13), 11,270–11,274, doi:10.1029/JB090iB13p11270.

Ludwig, K. R. (1989), PbDAT for MSDOS: A computer program for IBM-PC compatibles for processing raw Pb-U-Th isotope data, version 1.06, *U.S. Geol. Surv. Open File Rep.*, *88–542*.

Ludwig, K. R. (1990), ISOPLOT: A plotting and regression program for radiogenic isotope data, for IBM-PC compatible computers, version 2.02, *U.S. Geol. Surv. Open File Rep.*, *88–557*.

Ludwig, K. R. (2003), Isoplot 3.00: A geochronological toolkit for Microsoft Excel, *Spec Publ., 4*, Berkley Geochronol. Cent., Berkeley, Calif.

Marti, J., A. Geyer, A. Folch, and J. Gottsmann (2008), A review on collapse caldera modeling, in *Caldera Volcanism: Analysis, Modeling and Response*, edited by J. Gottsmann and J. Marti, pp. 233–283, Elsevier, New York, doi:10.1016/S1871-644X(07)00006-X.

Mattinson, J. M. (1973), Anomalous isotopic composition of lead in young zircons, *Carnegie Inst. Washington Year Book*, *72*, 613–616.

Mattinson, J. M. (2005), Zircon U/Pb chemical abrasion (CA-TIMS) method: Combined annealing and multi-step partial dissolution analysis for improved precision and accuracy of zircon ages, *Chem. Geol.*, *220*(1–2), 47–66, doi:10.1016/j.chemgeo.2005.03.011.

Matzel, J. E. P., S. A. Bowring, and R. B. Miller (2006), Time scales of pluton construction at differing crustal levels: Examples from the Mount Stuart and Tenpeak Intrusions, north Cascades, Washington, *Geol. Soc. Am. Bull.*, *118*(11–12), 1412–1430, doi:10.1130/B25923.1.

Menand, T. (2008), The mechanics and dynamics of sills in layered elastic rocks and their implications for the growth of laccoliths and other igneous complexes, *Earth Planet. Sci. Lett.*, *267*, 93–99, doi:10.1016/j.epsl.2007.11.043.

Menand, T. (2011), Physical controls and depth of emplacement of igneous bodies: A review, *Tectonophysics*, *500*, 11–19, doi:10.1016/j.tecto.2009.10.016.

Michel, J., L. Baumgartner, B. Putlitz, U. Schaltegger, and M. Ovtcharova (2008), Incremental growth of the Patagonian Torres del Paine Laccolith over 90 k.y., *Geology*, *36*(6), 459–462, doi:10.1130/G24546A.1.

Miller, J. S., J. E. P. Matzel, C. F. Miller, S. D. Burgess, and R. B. Miller (2007), Zircon growth and recycling during the assembly of large, composite arc plutons, *J. Volcanol. Geotherm. Res.*, *167*, 282–299, doi:10.1016/j.jvolgeores.2007.04.019.

Morgan, S., A. Stanik, E. Horsman, B. Tikoff, M. de Saint Blanquat, and G. Habert (2008), Emplacement of multiple magma sheets and wall rock deformation: Trachyte Mesa intrusion, Henry Mountains, Utah, *J. Struct. Geol.*, *30*(4), 491–512, doi:10.1016/j.jsg.2008.01.005.

Mundil, R., K. R. Ludwig, I. Metcalfe, and P. R. Renne (2004), Age and timing of the Permian mass extinctions: U/Pb dating of closed-system zircons, *Science*, *305*, 1760–1763, doi:10.1126/science.1101012.

Parrish, R. R., and T. E. Krogh (1987), Synthesis and purification of ^{205}Pb for U-Pb geochronology, *Chem. Geol.*, *66*(1–2), 103–110.

Petford, N., A. R. Cruden, K. J. W. McCaffrey, and J. L. Vigneresse (2000), Granite magma formation, transport and emplacement in the Earth's crust, *Nature*, *408*, 669–673, doi:10.1038/35047000.

Renne, P. R., J. I. Simon, R. Mundil, and K. R. Ludwig (2006), Implications of pre-eruptive zircon saturation in silicic magmas for high-precision U/Pb geochronology, *Eos Trans. AGU*, *87*(52), Fall Meet. Suppl., Abstract V21A-0564.

Roche, O., and T. H. Druitt (2001), Onset of caldera collapse during ignimbrite eruptions, *Earth Planet. Sci. Lett.*, *191*(3–4), 191–202, doi:10.1016/S0012-821X(01)00428-9.

Schmitz, M. D., and S. A. Bowring (2001), U-Pb zircon and titanite systematics of the Fish Canyon Tuff: An assessment of high-precision U-Pb geochronology and its application to young volcanic rocks, *Geochim. Cosmochim. Acta*, *65*(15), 2571–2587, doi:10.1016/S0016-7037(01)00616-0.

Simon, J. I., and M. R. Reid (2005), The pace of rhyolite differentiation and storage in an 'archetypical' silicic magma system, Long Valley, California, *Earth Planet. Sci. Lett.*, *235*, 123–140, doi:10.1016/j.epsl.2005.03.013.

Simon, J. I., M. R. Reid, and E. D. Young (2007), Lead isotopes by LA-MC-ICPMS: Tracking the emergence of mantle signatures in an evolving silicic magma system, *Geochim. Cosmochim. Acta*, *71*(8), 2014–2035, doi:10.1016/j.gca.2007.01.023.

Simon, J. I., P. R. Renne, and R. Mundil (2008), Implications of pre-eruptive magmatic histories of zircons for U-Pb geochronology of silicic extrusions, *Earth Planet. Sci. Lett.*, *266*, 182–194, doi:10.1016/j.epsl.2007.11.014.

Smith, R. L. (1979), Ash-flow magmatism, in *Ashflow Tuffs*, edited by C. E. Chapin, and W. E. Elston, *Spec Pap. Geol. Soc. Am.*, *180*, 5–27.

Steck, L. K., C. H. Thurber, M. C. Fehler, W. J. Lutter, P. M. Roberts, W. S. Baldridge, D. G. Stafford, and R. Sessions (1998), Crust and upper mantle P wave velocity structure beneath Valles Caldera, New Mexico: Results from the Jemez teleseismic tomography experiment, *J. Geophys. Res.*, *103*(B10), 24,301–24,320, doi:10.1029/98JB00750.

Steiger, R. H., and E. Jäger (1978), Subcommission on Geochronology: Convention on the use of decay constants in geochronology and cosmochronology, paper presented at 25th International Geological Congress, Geological Time Scale Symposium, Sydney, N. S. W., Australia.

Thompson, R. A., M. A. Dungan, and P. W. Lipman (1986), Multiple differentiation processes in early rift calc-alkaline volcanics, northern Rio Grande Rift, New Mexico, *J. Geophys. Res.*, *91*(B6), 6046–6058, doi:10.1029/JB091iB06p06046.

Tweto, O. (1979), The Rio Grande rift system, in *Rio Grande Rift: Tectonics and Magmatism*, edited by R. E. Riecker, pp. 33–56, AGU, Washington, D. C., doi:10.1029/SP014p0033.

Watson, E. B., and T. M. Harrison (1983), Zircon saturation revisited: Temperature and composition effects in a variety of crustal magma types, *Earth Planet. Sci. Lett.*, *64*(2), 295–304, doi:10.1016/0012-821X(83)90211-X.

White, S. M., J. A. Crisp, and F. J. Spera (2006), Long-term volumetric eruption rates and magma budgets, *Geochem. Geophys. Geosyst.*, *7*, Q03010, doi:10.1029/2005GC001002.

Wiebe, R. A., and W. J. Collins (1998), Depositional features and stratigraphic sections in granitic plutons: Implications for the emplacement and crystallization of granitic magma, *J. Struct. Geol.*, *20*(9–10), 1273–1289, doi:10.1016/S0191-8141(98)00059-5.

Wiebe, R. A., D. Smith, M. Strum, E. M. King, and M. S. Seckler (1997), Enclaves in the Cadillac Mountain Granite (costal Maine): Samples of hybrid magma from the base of the chamber, *J. Petrol.*, *38*(3), 393–423, doi:10.1093/petrology/38.3.393.